NASA Technical Memorandum 79225

(NASA-TM-79225) THE ROLE OF NaCl IN FLAME CHEMISTRY, IN THE DEPOSITION PROCESS, AND IN ITS REACTIONS WITH PROTECTIVE OXIDES AS RELATED TO HOT CORROSION (NASA) 27 p HC A03/MF A01 CSCL 07D G3/25

N79-28258

Unclas 31637

THE ROLE OF NaCl IN FLAME CHEMISTRY, IN THE DEPOSITION PROCESS, AND IN ITS REACTIONS WITH PROTECTIVE OXIDES AS RELATED TO HOT CORROSION

Fred J. Kohl, Carl A. Stearns,
and George C. Fryburg
Lewis Research Center
Cleveland, Ohio

Prepared for the
Fourth Conference on Gas Turbine Materials in a Marine Environment
Annapolis, Maryland, June 25-28, 1979

THE ROLE OF NaCl IN FLAME CHEMISTRY, IN THE DEPOSITION PROCESS, AND IN ITS REACTIONS WITH PROTECTIVE OXIDES AS RELATED TO HOT CORROSION

Fred J. Kohl, Carl A. Stearns, and George C. Fryburg

NASA-Lewis Research Center
Cleveland, Ohio 44135 USA

SUMMARY

This paper reviews the results of some NASA-Lewis Research Center programs directed toward obtaining an understanding of the chemistry of NaCl in the combustion process, in the deposition process, and in its reactions with surface oxides. Sodium chloride is believed to be the primary source of turbine engine contamination that contributes to hot corrosion. The behavior of NaCl-containing aerosols ingested with turbine intake air is very complex; some of the NaCl may vaporize during combustion while some may remain as particulates.

The NaCl can lead to Na_2SO_4 formation by several possible routes or it can contribute to corrosion directly. Hydrogen or oxygen atom reaction with NaCl(c) has been shown to result in the release of Na(g). Gaseous NaCl in flames can be partially converted to gaseous Na_2SO_4 by homogeneous reactions. The remaining gaseous NaCl and other Na-containing molecules can act as sodium carriers for condensate deposition of Na_2SO_4 on cool surfaces. A frozen boundary layer theory has been developed to predict the rates of deposition. Condensed phase NaCl can be converted directly to condensed Na_2SO_4 by reaction with sulfur oxides and O_2. Reaction of gaseous NaCl with Cr_2O_3 results in the vapor phase transport of chromium by the formation of complex Cr-containing gaseous molecules. Similar gaseous complexes are formed with molybdenum. The presence of gaseous NaCl has been shown to affect the oxidation kinetics of Ni-Cr alloys; it also causes changes in the surface morphology of Al_2O_3 scales formed on Al-containing alloys.

INTRODUCTION

The reaction of sodium chloride (one of the main constituents of sea salt) with sulfur oxides leads to deposits of sodium sulfate, Na_2SO_4, in gas turbine engines. It has also been established that sodium chloride alone, or in combination with sodium sulfate, can cause severe hot corrosion of gas turbine components. Numerous studies in the past have been directed toward examining the physical behavior of the NaCl-containing aerosol as it passes through the gas turbine engine's compressor, combustor, and turbine sections (e.g., Refs. 1 to 3). In addition, the chemical mechanisms of the reactions between these condensed phase corrosive salts and the nominally protective surface oxides on component materials (superalloys and coatings) has been investigated extensively (e.g., Refs. 4 to 10). Many studies of this type have been reported at the previous three Conferences on Gas Turbine Materials in a Marine Environment (Refs. 11 to 13). Complementary to the studies of NaCl in relation to turbine engine chemistry, the role of NaCl in coal-fired boiler systems has also been examined

in the past (e.g., Refs. 14 to 22).

At the NASA-Lewis Research Center, various in-house and contract or grant-supported studies have been directed toward understanding the fundamental chemistry of NaCl in the combustion process, in the deposition process, and in the reactions with component surface oxides. A better understanding of the physicochemical behavior of all of the components participating in the high temperature corrosion process should help guide material improvements and/or lead to control strategies that will minimize or alleviate the problem.

The combustion process has been studied by high pressure mass spectrometric sampling of NaCl/sulfur-doped laboratory flames (Refs. 23 to 25). The experimental results were compared with equilibrium thermochemical calculations of combustion gas compositions. The reactions between NaCl(c) and H or O atoms have also been examined (Refs. 26 and 27). Furthermore, the deposition of Na_2SO_4 on cooled collectors has been studied by seeding a Mach 0.3 burner rig with NaCl or sea salt (Ref. 28). A multicomponent mass transfer theory has been developed to predict the rate of deposition via vapor transport (Refs. 29 and 30). In parallel with the gaseous reaction studies, the kinetics of conversion of condensed phase NaCl to Na_2SO_4 by reaction with SO_2 and O_2 was also examined. In addition to these basic studies on the Na_2SO_4/NaCl system, several techniques, including mass spectrometry, have been employed in order to elucidate the reactions between NaCl(g) and the various metal oxides formed on turbine alloy surfaces (Refs. 31 and 32). Such reactions have been observed to result in the vapor phase transport of some of these metals away from the component surfaces. Lastly, the effects of gaseous NaCl on the oxidation kinetics and surface morphology of some chromia- and alumina-forming alloys have been studied (Refs. 33 to 36).

This paper surveys and reviews some of the recent results of these programs.

COMBUSTION CHEMISTRY

Until recently, there was considerable speculation regarding the molecular composition of sodium-containing species in flames and the kinetics of the gas phase formation of sodium sulfate. Generally it had been assumed that sulfur impurities in the fuel and sodium chloride in the ingested air react during combusion to yield gaseous sodium sulfate by overall reactions of the type:

$$2\ NaCl(g) + SO_2(g) + \tfrac{1}{2}\ O_2(g) + H_2O(g) = Na_2SO_4(g) + 2\ HCl(g) \qquad (1)$$

$$2\ NaOH(g) + SO_2(g) + \tfrac{1}{2}\ O_2(g) = Na_2SO_4(g) + H_2O(g) \qquad (2)$$

A recent Lewis Research Center high temperature Knudsen cell investigation of the vaporization of sodium sulfate (Ref. 37) has lent credence to such reactions by establishing the existence of the $Na_2SO_4(g)$ molecule and by providing values for its thermodynamic properties (Ref. 38). To obtain a greater understanding of the chemistry of hydrocarbon flames doped with sulfur and sodium salts, high pressure sampling mass spectrometry has been used to measure the composition of combustion products in several laboratory flames (Refs. 23 to 25). The experimental results were compared with equilibrium thermodynamic

calculations of combustion gas composition.

Flame Compositions

Flame Sampling by Mass Spectrometry.-Premixed fuel-lean methane/oxygen flames were burned on a laminar flow, flat flame burner which is illustrated in Figure 1 (Refs. 23 to 25). Sulfur was added to the gas mixtures as either SO_2 or CH_3SH. In addition, the gas mixtures could be seeded with alkali salts (e.g., NaCl or Na_2CO_3) by nebulizing aspirated water solutions into the mixing chamber of the burner. A typical flame had a luminous zone located somewhat less than one millimeter above the top surface of the burner and a thickness of about one millimeter. The burner was supported by a mechanical device so that the vertical distance between burner and sampler, perpendicular to the flame front, could be varied. Composition profiles were obtained by measuring the various gaseous species as a function of distance from the burner surface (or residence time), through the flame and into the post-flame region.

Direct mass spectrometric analysis of the species present in atmospheric pressure flames was accomplished with a high pressure, free-jet expansion, modulated molecular beam mass spectrometric sampler. A schematic diagram of the experimental arrangement is also shown in Figure 1. This technique allows one to sample all the gas phase species directly while preserving their dynamic and chemical integrity (i.e., frozen chemistry).

The theory and a description of the sampler have been presented elsewhere (Ref. 39). Briefly, the gas enters the sampler through a Pt-10%Rh orifice located in the apex of a sampling cone. The gas is expanded as a free jet, converted to a molecular beam and passed, via differentially pumped vacuum stages, into a quadrupole mass spectrometer operated at pressures below 10^{-8} torr. The molecular beam is modulated by a rotating segmented disc and synchronous detection is used to measure ion currents resulting from ions produced by electron bombardment of the neutral molecular beam.

Results are given in Figure 2 for a CH_4/O_2 flame doped with SO_2 and seeded with an aspirated solution of NaCl. The flame speed was 42 cm sec^{-1}. The most significant observations are (1) the gaseous Na_2SO_4 molecule was formed; (2) the residence time required for formation of $Na_2SO_4(g)$ was less than one millisecond; (3) not all of the NaCl was converted, that is, gaseous NaCl persists in the flame; (4) sodium- sulfur-containing intermediate species $NaSO_2(g)$ and $NaSO_3(g)$ were identified; and (4) the expected permanent gaseous products were identified.

Calculations of Flame composition.-To facilitate a comparison of experimental observations with equilibrium thermodynamic predictions, the mole fractions of flame reaction products were calculated (Refs. 23 to 25). The calculations were made with the widely used NASA complex chemical equilibrium computer program (Ref. 40). This program is based on the minimization of free energy approach to chemical equilibrium calculations, subject to the constraint of maintaining a proper mass balance between reactants and products. The program permits calculation of chemical equilibrium compositions in homogeneous or heterogeneous systems for assigned thermodynamic states such as

temperature-pressure (T,P) and enthalpy-pressure (H,P).

The role of NaCl in methane/oxygen flames was examined by obtaining flame temperatures and compositions as a function of fuel/oxidant mass ratio. In the calculations, the convention used was that CH_4 and SO_2 were labeled fuel and O_2, H_2O, and NaCl were labeled oxidant. The calculated equilibrium compositions of the reacted flame gas products at the adiabatic flame temperatures are presented in Figure 3 as a function of fuel/oxidant ratio. The major products are in the first plot and the sodium-containing species are in the second. To arrive at the distribution of molecular species depicted in Figure 3, the program considered over 70 gaseous and condensed phase species made up of C-H-O-S-Na-Cl combinations. Note that only those molecular species for which the program was given thermodynamic data were considered in the calculations; no data for $NaSO_2$ or $NaSO_3$ were included.

The results of the calculations showed that the sodium is distributed in a complex pattern between $Na_2SO_4(c)$, NaCl(g), NaOH(g), $Na_2SO_4(g)$, Na(g), $(NaCl)_2(g)$, NaO(g), and NaH(g). At low values of the fuel/oxidant ratio (corresponding to low flame temperatures), and up to a sharp cut-off point, the sodium is tied up almost exclusively in the condensed phase as $Na_2SO_4(c)$. Based on the calculations, gaseous Na_2SO_4 can be expected to be present in significant amounts only over a relatively narrow fuel/oxidant ratio range and would always be present at a molar concentration of less than one-tenth that of NaCl(g). At high fuel/oxidant ratios, NaOH(g), Na(g), and NaCl(g) were calculated to account for most of the sodium.

Experimental results can be compared with the calculated results shown in Figure 3 by noting that, according to the fuel and oxidant convention used, the fuel/oxidant mass ratio for the experimental flame was 0.072. For ease of comparison, calculated mole fractions of product species for this ratio are shown on the right-hand side of Figure 2. At the outset one must recognize that the following two factors affect this comparison: (1) The experimental results were not "calibrated" for various mass spectrometric sensitivity factors and (2) The calculations are for equilibrium conditions only, at the adiabatic flame temperature. With these factors in mind, the agreement between experiment and calculation is considered to be good for all of the species except NaCl and Na_2SO_4. Several reasons may account for the disagreement between experiment and calculations for these two particular species: (1) The sodium level in the flame has uncertainty associated with it due to the method used to introduce the sodium chloride; (2) The concentration of $Na_2SO_4(g)$ is a rapidly varying function of temperature and fuel/oxidant ratio; and (3) The true flame temperature is expected to be significantly below the calculated adiabatic flame temperature of 2032K. We have calculated that if the flame were 200K cooler, the predicted level of $Na_2SO_4(g)$ would equal the experimental level. By reflecting on all of the factors above, we concluded that the agreement between experiment and calculation is reasonably good. Thus calculations can be useful in predicting, at least qualitatively, what is to be expected in experimental doped flame systems.

$NaCl(g)/SO_2/H_2O/O_2$ Reaction

The reaction between gaseous NaCl, O_2, SO_2, and H_2O has been studied by mass spectrometrically sampling the gases from a reaction tube through which the mixture flowed (Ref. 23). The residence time in the reactor was about two seconds. The product species $Na_2SO_4(g)$, $SO_3(g)$, and $NaSO_3(g)$ were observed as illustrated in Figure 4. The relative concentrations of each species, including $Na_2SO_4(g)$ and $SO_3(g)$ compared well with those calculated by equilibrium thermodynamics. These measurements further demonstrate that equilibrium is readily achieved in such a gas mixture at temperatures above 1000K.

Reactions of NaCl(c) with Hydrogen and Oxygen Atoms

It is generally believed that, in flames, NaCl(c) first vaporizes and its sodium is released via gas phase reactions between the resultant NaCl vapor and atomic hydrogen (Ref. 41). However, for large particles, the residence time in the combustor may be insufficient for complete vaporization (Ref. 3). Thus the possibility arises that heterogeneous reactions may contribute to sodium release. The kinetics of such reactions, or important rivals to them, have not previously been explored in any detail.

As part of an NASA-sponsored program to elucidate the basic kinetics and mechanisms of these processes, Professor D. E. Rosner and Dr. P. D. Foo at Yale University have been examining heterogeneous reactions between solid NaCl and atomic hydrogen or oxygen (Refs. 26 and 27):

$$H(g) + NaCl(s) \rightarrow Na(g) + HCl(g) \quad (3)$$

$$O(g) + NaCl(s) \rightarrow Na^*(g) + ClO(g) \quad (4)$$

Because of the importance of gaseous Na as a possible precursor to $Na_2SO_4(c)$ formation, data on these reactions should allow the evaluation of alternate mechanisms to those involving NaCl vaporization.

A kinetic and stoichiometric study of reaction (3) was carried out by using atomic absorption spectroscopy (to detect Na atoms) combined with microwave discharge-vacuum flow reactor techniques (to produce H atoms) over the temperature range 540 to 680K. The preliminary results (Ref. 26) indicated that H-atom attack of solid NaCl indeed produces Na-atoms even at these low temperatures. Because at the low temperature, NaCl vaporization is negligible, the corresponding homogeneous gas phase reaction

$$H(g) + NaCl(g) \rightarrow Na(g) + HCl(g) \quad (5)$$

plays no role in the Na(g) production observed in these studies. By combining the absorbances measured for Na(g) in the Arrhenius rate expression with the Lambert-Beer Law, the apparent activation energy for reaction (3) of 5.2 kcal $mole^{-1}$ was obtained.

Reaction (4) was studied (Ref. 26) by using emission spectroscopy (to detect Na*(g), combined with microwave discharge techniques (to generate O-atoms) in an O_2/Ar gas mixture. Even though the thermodynamics for this reaction would seem to be less favorable than those for reaction (3), Na*(g) was readily detectable between 510 and 620K. An Arrhenius treatment of the data for this reaction yielded an activation energy of 9.4 kcal $mole^{-1}$.

The fact that the reactions between solid NaCl and atomic hydrogen and oxygen exhibit such low activation energies is important in understanding the behavior of sodium in flame chemistry. High concentrations of H and O atoms exist in the reaction zone of hydrocarbon/air flames. The high diffusivity of the H atom makes reaction (3) seem to be particularly important as a mechanism for Na release and indicates that Na(g) may be released very early in the combustion process by a heterogeneous reaction. This process has thus freed Na atoms which can subsequently react to form other stable products without going through the route of sodium chloride vaporization.

DEPOSITION PROCESS

The deposition of sodium sulfate from combustion gases containing sodium and sulfur is regarded as one of the fundamental steps in the phenomenon of hot corrosion of turbine components. Even though the primary concern of this paper is the chemistry of NaCl, it is through the formation and deposition of Na_2SO_4 that NaCl has its predominant effect in hot corrosion. Recently, we described (Ref. 37) an equilibrium thermodynamic method of predicting condensation onset temperatures (dew points) of Na_2SO_4 in flame environments as a function of sulfur in the fuel and sea salt concentration in the intake air. The method consisted of applying the NASA complex chemical equilibrium computer program (Ref. 40). Thermodynamic properties of gaseous and condensed phase Na_2SO_4, along with additional species pertinent in sea salt-containing environments, were used in the program to calculate equilibrium combustion gas compositions and temperatures for representative turbine engine and burner rig flames. Compositions were calculated for various fuel/oxidant ratios with different concentrations of sulfur in the fuel and different concentrations of sea salt added to the intake air. Calculations were made to determine the temperature below which condensation of Na_2SO_4 should be expected.

Deposition Experiments

To validate the thermochemical dew point predictions and to provide the basis for development of a deposition rate theory, experiments have been carried out by using a Mach 0.3 atmospheric pressure burner rig as shown in Figure 5 (Ref. 28). A characteristic of the burner rig that was important in this study was the residence time of the dopant in the flame. Residence time is defined as the time interval between introduction of the salt-containing aerosol into the burner and the arrival of the salt at the collector. Calculations based on the geometry of the rig and the gaseous flow velocity revealed that the residence time was 2.2 milliseconds. The burner used

Jet A-1 fuel. The air was seeded with about 10 wppm of an inorganic sodium salt (NaCl, sea salt or Na_2SO_4). Deposits were collected on a cylindrical platinum target situated in the combustion gases. The deposition rate was determined at different collector target temperatures. It was anticipated that accuracy of theoretical predictions for a burner rig environment would lend credence to eventual predictions for actual turbine engine conditions, and to specifications for operating parameters necessary for more realistic burner rig simulation of engine conditions.

The results of the experiments that used sea salt and NaCl seeding are given in Figures 6 and 7. Chemical analysis, X-ray diffraction, and energy dispersive spectrometry analysis showed that the deposits consisted of mainly Na_2SO_4 with minor amounts of K_2SO_4, $CaSO_4$, and MgO from the sea salt runs; they consisted of pure Na_2SO_4 from the NaCl runs. An SEM micrograph of a deposit from a sea salt experiment, shown in Figure 8, disclosed that the deposit consisted of crystalline needles protruding from a fibrous mat. The appearance of the crystals indicates that the deposition occurred by vapor deposition of molecules, and not by impaction or capture of particles. Chemical analysis of the water solutions leached from the targets revealed that no soluble Cl^- was present in the deposits above background levels. Thus the chemical identification of the deposit composition was in agreement with the predictions of the chemical equilibrium computer program. The experimental condensation onset temperatures also agreed within the experimental uncertainties (±15K) with the predicted temperatures calculated from thermochemical data.

The observation that Na_2SO_4 deposition was obtained in a residence time on the order of 2.2 milliseconds is significant. This observation, and those from the flame sampling studies are in apparent disagreement with the observations of Hanby (Ref. 42) that residence times of greater than eight milliseconds were required for formation of Na_2SO_4 in combustion gases. A critical analysis of Hanby's results is complicated by the difficulty of determining the fuel/air ratio in different sections of his combustor. Apparently, Na_2SO_4 was detected only after the fuel/air ratio of the combustion products was changed by the addition of dilution cooling air. This situation makes definition of the residence time uncertain.

Deposition Theory

During the course of this research, it became obvious that a theoretical prediction was desirable for the rates of deposition of $Na_2SO_4(c)$ at surface temperatures below the deposition onset temperature. Toward this end, a comprehensive yet tractable mass transfer equation was developed for making such predictions by an NASA-sponsored collaborative effort between Professor D. E. Rosner and associates at Yale University and NASA personnel (Refs. 28 to 30). The experimental data obtained from the burner rig experiments provided a useful basis for developing and validating a deposition rate theory. It should be noted, however, that a gas turbine engine is a much more complicated system than the burner rig described here. The engine operates at significantly higher pressure and mass flow, and with complex

mixing of fuel and air in the different sections. Thus, the applicability of the developed theory to engines remains to be demonstrated.

The experimental existence of a "dew point" surface temperature above which no deposition of Na_2SO_4(c) was observed suggested to us that under the burner rig test conditions, deposition was associated with vapor diffusion to the collector across a "boundary layer." Accordingly, a convective diffusion theory employing multicomponent vapor transport for predicting Na_2SO_4 deposition rates in the burner rig experiments has been developed. However, the resultant theory is also sufficiently general to be able to include transport by particles small enough to behave like heavy vapor molecules. In the theory development, two simplifying assumptions have been made: (1) All sodium added to the combustion gases is available for transport to the target via vapor species and (2) While local thermochemical equilibrium is achieved at the outer and inner edges of the concentration boundary layer around the collector, no homogeneous chemical reactions occur within the diffusion boundary layer. Thus the boundary layer is said to be chemically "frozen." This latter assumption markedly reduces computational time. The theory is referred to as the chemically frozen boundary layer (CFBL) theory.

In contrast to previous treatments of vapor deposition (Refs. 3 and 43 to 45), the CFBL theory makes provision for the effects of: (1) Na-element transport via species of differing mobility (i.e., NaCl(g), NaOH(g), Na(g), Na_2SO_4(g)); (2) thermal (Soret) diffusion of heavy, Na-containing species; and (3) free stream turbulence intensity and scale. The formulation of the CFBL theory is presented in References 28 and 29.

The results of the application of the CFBL theory to the prediction of deposition rates for the sea salt and NaCl-seeded burner rig experiments are given in Figures 6 and 7. Agreement between maximum deposition rates far below the dew point (ca. 5 mg/hr.) predicted by the theory and those obtained in the experiments is good, but the predicted dependence on surface temperature exhibits plateau-like behavior not evident from the experiments. Nonetheless, the agreement is particularly encouraging in view of the fact that the burner rig was being seeded heavily with Na-compounds at the gram per hour level. The theory has also been used to predict the form of the dependence of the deposition rate on fuel sulfur content and on pressure level (Refs. 29 and 30).

While condensed phase Na_2SO_4 can be formally regarded as one of the diffusing species, in practice, our knowledge of the particle size distribution (hence Browian and thermophoretic diffusion parameters) is presently inadequate to assess this contribution to the observed deposition rates. For this reason, and because of the highly undersaturated state of our seeded combustion products upstream of the target, only vapor diffusion has been included in our treatment up to the present time.

By examining the nature of the equilibrium calculated species concentrations in the combustion gas free stream and at the surface of the collector, some insight may be gained regarding the nature of the transporting species in the context of the CFBL theory. According to this model, Na_2SO_4(c) growth on a surface occurs primarily via transport of NaOH(g), NaCl(g), and

Na(g), not Na_2SO_4(g). In fact, the Na_2SO_4(g) species contributes to a net loss (not gain) of the condensate layer, due to a negative concentration gradient for this species across the boundary layer. Thus in the CFBL framework, gas phase conversion of NaCl to Na_2SO_4 in the available residence time is not necessary for the process of Na_2SO_4 deposition. Rather, of more importance are heterogeneous reactions at the gas/liquid interface which convert NaCl(g), NaOH(g), and Na(g) to Na_2SO_4(l) in the presence of excess O_2 and S-containing vapor species. Of course, the mechanism of this conversion may involve an Na_2SO_4 molecule. This situation makes it clear that a multicomponent deposition theory is absolutely essential in engineering applications.

An interesting aspect of calculations of combustion gas and deposit compositions was consideration of what condensed phases, other than Na_2SO_4, might be expected to deposit from sodium-seeded combustion gases. Na_2SO_4 was the only condensate expected over a wide range of temperatures with an equivalence ratio of less than one (oxidizing conditions). Under the conditions investigated, the calculations predict that no NaCl or NaOH condensates form. Even if Na_2SO_4(c) were prohibited from forming (by omitting data for this phase from the program library) no NaCl or NaOH condensates would form. Our calculations show that the phase that would likely form from a thermodynamic viewpoint would be Na_2CO_3, which is much more stable in a combustion gas environment than NaCl(c).[2] The high stability of the chlorine-containing HCl molecule is also important here. This phenomenon is an illustration that even though a molecule with a certain stoichiometry (such as NaCl) is one of the more stable gases in a complex equilibrium, the same composition may not be the most stable condensed phase. Indeed, the deposition of Na_2CO_3 has been observed from Na-seeded sulfur-free propane/air flames (Ref. 46). Thus it is not surprising that in practice NaCl is rarely detected as a condensed phase deposit in turbine engines or burner rigs. Situations in which NaCl deposits were observed (Refs. 16, 17, 19, 21, and 47), at levels greater than those predicted by Raoult's Law (Ref. 52), must be attributed to particle capture.

Condensed Phase NaCl to Na_2SO_4 Conversion

Because it should be possible for NaCl to deposit by particle impaction, one might expect chloride to be found in the hot section of turbines. However, it is rarely detected or is only present at very low levels (e.g., Refs. 2 and 48). The question arises whether the cause for this observation is that NaCl(c) reacts with SO_2 and O_2 to form Na_2SO_4(c) and a gaseous Cl-containing molecule. A knowledge of the kinetic parameters for this process would be useful in interpreting the subsequent behavior of NaCl particles which have deposited by impaction. The basic chemistry of the conversion reaction is being investigated thermogravimetrically by the authors and W. L. Fielder of NASA. The reaction of single crystal NaCl with slowly flowing mixtures of SO_2 in O_2 at 1 atmosphere total pressure is being studied.

Preliminary results over the temperature range of 600 to 900K for the reaction with an initial concentration of 8 mole % SO_2 in O_2 are shown by an Arrhenius-type plot in Figure 9. The data points shown were obtained from

a number of individual NaCl single crystals and have been combined into one plot. The activation energy calculated from the data in Figure 9 is 12 kcal mole^{-1}. This low value indicates that the NaCl to Na_2SO_4 conversion can take place readily even at moderate temperatures, and this may explain the observation that Cl^- is rarely detected in deposits from combustion systems. Thermodynamics predicts that essentially no condensed phase NaCl should exist. Of course, a small amount of NaCl should dissolve in Na_2SO_4 according to Raoult's Law for solutions. The low activation energy observed for the reaction indicates that only small kinetic barriers exist to prevent the chemical equilibrium from being achieved.

Interaction of NaCl(g) and HCl(g) with Na_2SO_4

Several investigators have reported that NaCl(g) apparently acted to induce dissociation or vaporization of Na_2SO_4(c) (e.g., Refs. 49 to 51). Thus the interaction of Na_2SO_4(l) with NaCl(g), HCl(g), and H_2O(g) was studied in atmospheric pressure flowing air and oxygen at Na_2SO_4(l) temperatures of 900 and 1000K (Ref. 52). Thermogravimetric and high pressure mass spectrometric sampling techniques were used in the investigation. The experimental results established that previously reported enhanced rates of weight loss of Na_2SO_4(l) in the presence of NaCl(g) are due to the reaction

$$2\ NaCl(g) + SO_2(g) + H_2O(g) + \tfrac{1}{2}\ O_2(g) = Na_2SO_4(l) + 2\ HCl(g) \qquad (6)$$

being driven to the left in flowing gas systems. The loss of SO_2 from the system results in a net loss of Na_2SO_4 and because SO_2 is not being replaced as a reactant, the amount of Na_2SO_4(l) in the system decreases. The HCl(g) needed to drive the reaction to the right is formed by the hydrolysis of NaCl caused by small but significant amounts of H_2O(g) present in most experimental systems (and always present in combustion gases) by the reaction

$$NaCl(g) + H_2O(g) = NaOH(g) + HCl(g) \qquad (7)$$

Supplementing the experimental observations are thermochemical calculations which show that even with sub-ppm levels of H_2O(g) present, significant quantities of HCl(g) should be produced.

REACTIONS WITH OXIDES

Equilibrium thermodynamic calculations indicate that the engine hot section, under conditions conducive to hot corrosion, should be relatively rich in the contaminant gases NaCl, NaOH, and HCl (Ref. 37). These chemical species are generally considered as highly reactive at high temperatures, and therefore it seems reasonable to expect that they might play a significant role in the hot corrosion process. Previously it had been demonstrated that adverse effects could be associated with exposure of hot oxidizing metals to partial pressures of NaCl(g) (e.g., see Refs. 51 and 53 to 56). The major effects observed were: (1) NaCl(g) could compromise the so-called protective oxide scale on certain superalloys by degrading the oxide adherence which resulted in spalling; (2) NaCl(g) removed chromium from samples as a volatile

chromium compound; and (3) NaCl(g) could accelerate the degradation, by sulfidative oxidation, of certain CoCrAlY-coated alloys (Ref. 51). Thus several NASA-sponsored programs have concentrated on elucidating the high temperature chemistry of NaCl(g) in regard to corrosion-related processes.

In addition to gas phase NaCl, solid or liquid NaCl may come into contact with oxide surfaces in turbines. It has been shown (Ref. 2) that compressors of gas turbine engines can physically collect some solid sodium chloride and sulfate from the sea salt aerosol. These deposits can be periodically shed from the compressor and pass to the hot section of the turbine. The particles may then vaporize, react, impact on turbine surfaces, or pass through the engine. It has been well established that condensed NaCl or $NaCl-Na_2SO_4$ mixtures can be very corrosive (e.g., see Refs. 9 and 57 to 60). However, to date, such studies have not been a part of the NASA program.

Volatile Products Studies

Cooled target vapor collection techniques were used to study the formation of volatile products when samples of Cr, Mo, and several superalloys were exposed at elevated temperatures to oxidizing environments containing NaCl(g) and $H_2O(g)$ (Refs. 31 and 32). High pressure mass spectrometric sampling was used to identify directly the volatile product molecules emanating from these materials. Schematics of the respective apparatus are shown in Figure 10. The metal samples were suspended in a furnace and mixtures of O_2 and NaCl(g) with and without added $H_2O(g)$ were slowly passed over the samples. In the target collection experiments, volatile products were condensed on water-cooled platinum targets, subsequently dissolved in water, and the resulting solutions analyzed for metal cations by atomic absorption and/or emission spectroscopy. The identification of the volatile species was accomplished with the high pressure mass spectrometric sampler.

The target collection experiments with chromium showed that the rate of transport of chromium as a volatile species was significantly enhanced when $H_2O(g)$ and/or NaCl(g) was added to the oxidizing environment. The experiments are discussed in References 31 and 32. For chromium and chromia-forming alloys, the volatile species were identified by mass spectrometry as being primarily $(NaCl)_x CrO_3$ where X = 1, 2, or 3 and $(NaOH)_y CrO_3$ where y = 1 or 2. The mass spectral data that lead to these identifications for this system are shown in Figure 11. Similar results were obtained at lower temperatures (~675°C) for molybdenum where the major species identified were $(NaCl)_y(MoO_3)_3$ and $NaOH(MoO_3)_3$. We believe that the complex vapor species observed in our studies were the first examples of such gaseous alkali halide-metal oxide complexes. In this regard, one point must be emphasized: the fact that the rate of transport of chromium was found to increase in the target experiments when NaCl(g) was added to the system $Cr_2O_3(g) + O_2(g)$ indicates that the rate is not limited by the vaporization rate of $CrO_3(g)$. The only volatile species formed in the absence of NaCl(g) was $CrO_3(g)$. Therefore, the Na/Cr-containing species are not products of homogeneous gas phase reactions but are formed by heterogeneous reactions. Furthermore, because species such as $(NaCl)_x CrO_3$ are not the product of gas phase reactions, they likewise cannot be the product of sampling

artifacts such as clustering or beam condensation in the high pressure sampler.

An exhaustive search was made for the frequently proposed vapor molecules CrO_2Cl_2, $CrCl_2$, $CrCl_3$, and Na_2CrO_4. This effort was unrewarding and only the species $Na_2Cr_2O_7(g)$ was detected in addition to the previously identified chemical complexes. However, this is not to say that some of the aforementioned species will not form under other conditions, e.g., at low oxygen pressure, in a vacuum, or in the absence of sodium. Certainly it is expected that $Na_2CrO_4(g)$, which has been identified as a stable molecule in vacuum by a Knudsen cell-mass spectrometry study (Ref. 61), would form when Na_2SO_4 reacts with Cr_2O_3 in O_2 in the absence of any chlorine.

We have concluded that the main reactions responsible for the vapor transport of chromium in various situations are:

$$\tfrac{1}{2}\ Cr_2O_3(c) + 3/4\ O_2(g) = CrO_3(g) \tag{8}$$

$$\tfrac{1}{2}\ Cr_2O_3(c) + 3/4\ O_2(g) + H_2O(g) = CrO_2(OH)_2(g) \tag{9}$$

$$\tfrac{1}{2}\ Cr_2O_3(c) + 3/4\ O_2(g) + xNaCl(g) = (NaCl)_xCrO_3(g),\ x = 1,\ 2,\ \text{or}\ 3 \tag{10}$$

$$\tfrac{1}{2}\ Cr_2O_3(c) + 3/4\ O_2(g) + xNaOH(g) = (NaOH)_xCrO_3(g),\ x = 1\ \text{or}\ 2 \tag{11}$$

Various kinetic parameters for Reactions (8) and (10) are reported in Reference 31. For molybdenum, the main reactions responsible for the vapor phase transport were deduced to be:

$$xMoO_3(c) = (MoO_3)_x(g),\ x = 3\ \text{or}\ 4 \tag{12}$$

$$MoO_3(c) + H_2O(g) = MoO_2(OH)_2(g) \tag{13}$$

$$3\ MoO_3(c) + xNaCl(g) = (NaCl)_x(MoO_3)_3(g),\ x = 1\ \text{or}\ 2 \tag{14}$$

$$3\ MoO_3(c) + NaOH(g) = NaOH(MoO_3)_3(g) \tag{15}$$

The molecules that were identified are felt to be the ones responsible for the vapor phase transport of the respective metals in corrosive salt-containing atmospheres. They appear to be more thermodynamically stable under oxidizing conditions in the presence of NaCl(g) than the other previously postulated species.

It is intriguing to postulate what the role of the complex vapor molecules might be in the corrosion process. Thinning of a chromium oxide scale could result in the formation of regions of aggravated stress where cracking might occur, thus compromising the scale. Also, a thinned section of scale might be more readily breached or fluxed by $Na_2SO_4(c)$. In either case, NaCl(g) attack compromises the oxide scale and thus promotes hot corrosion attack. It is important to emphasize that although the degree of attack by NaCl(g) is of a much smaller magnitude than the $Na_2SO_4(c)$ hot corrosion attack, the NaCl(g) attack may be of comparable importance in the overall high

temperature corrosion process taking place in turbine engines.

Effect of NaCl(g) on Oxidation and Hot Corrosion of NiAl and NiCr

To complement the volatile species studies described directly above, J. G. Smeggil and N. S. Bornstein of United Technologies Research Laboratories have investigated, under NASA Contract No. NAS3-20039, the effect of NaCl(g) on the oxidation and Na_2SO_4-induced hot corrosion of NiAl and several chromia-forming alloys. The results of these studies are given in References 33 to 36.

In brief, the thermogravimetric oxidation studies and extensive metallography have demonstrated an effect of NaCl(g) on the oxidation of NiAl (Refs. 33 and 35). Even at low concentrations, NaCl vapor substantially modifies the high temperature oxidation behavior of the alumina-former NiAl. The role of the NaCl(g) is two-fold. Firstly, aluminum is removed from a dense protective Al_2O_3 scale and redeposited on the surface of the scale as Al_2O_3 whiskers. This startling effect is illustrated in Figure 12. Secondly, the NaCl vapor effects isothermal spallation of the normally protective Al_2O_3. The interaction of NaCl(g) with NiAl is not expected to be unique and likely occurs with other alumina-forming surface coatings and substrate compositions. At this time, the mechanism of whisker growth and spalling is not completely understood, although vapor phase and grain boundary diffusion might account for the observations.

In the incubation period associated with Na_2SO_4-induced hot corrosion of NiAl, NaCl(g) has been shown to be effective in removing aluminum from below the protective alumina scale and redepositing it as Al_2O_3 whiskers on the surface of the Na_2SO_4-coated sample (Refs. 33 and 36). The removal of aluminum from below the surface of the oxide layer locally depletes the substrate of aluminum and leads to a progressive weakening of the protective scale-substrate bond. Upon rupture of the protective Al_2O_3 scale, the substrate locally has an insufficient aluminum activity to reform the protective layer. At low temperatures, the diffusion rates are not high enough to allow aluminum to reform the protective Al_2O_3 scale. This condition has been shown in oxidation studies to be sufficient to cause accelerated oxidation rates.

The oxidation behavior of elemental chromium and Ni-25Cr have been studied at 900 and 1050°C in oxygen atmospheres with and without the addition of gaseous NaCl (Refs. 33 and 34). Effects arising from the presence of small concentrations of NaCl(g) are reflected both in thermogravimetric data as illustrated in Figure 13 and in the microstructure of the oxide scales formed. For Ni-25Cr, "S"-shaped oxidation curves are obtained when NaCl(g) is present in the oxidizing environment. This curve shape suggests breakaway oxidation kinetics for Ni-25Cr with NaCl(g) while no such breakaway is seen for pure chromium. The removal of chromium from chromia scales on Ni-25Cr affects the formation of a zone depleted of chromium in the alloy substrate adjacent to the scale. With the consequently reduced activity of chromium

thermodynamic considerations favor the formation of the spinel $NiCr_2O_4$. Thus the breaks observed in the thermogravimetric data are taken to represent and correspond to the conversion of the scale from the protective chromia to the somewhat less protective spinel.

CONCLUDING REMARKS

As illustrated in Figure 14, the behavior of the NaCl-containing aerosols ingested into turbine engines with the intake air is very complex. Some of the NaCl may vaporize while some may remain as particulates. NaCl(c or g) can lead to Na_2SO_4 formation by several possible routes or it can contribute to corrosion directly.

The chemical studies reviewed here have elucidated the possible roles that sodium chloride can play in the overall hot corrosion process. Besides being a source of sodium for formation of the corrosive liquid sodium sulfate, the sodium chloride itself contributes in other ways to the overall process of material degradation. The understanding gained of the sodium chloride involvement chemistry has provided valuable insights into better testing procedures and strategies for alleviating the hot corrosion problem.

REFERENCES

1. I. I. Bessen and R. E. Fryxell, in "Gas Turbine Materials Conference Proceedings," p. 73, Naval Ship Engineering Center, Naval Air Systems Command, Washington, DC, 1972.

2. R. E. Fryxell and I. I. Bessen, in "Proceedings of the 1974 Gas Turbine Materials in the Marine Environment Conference," p. 259, J. W. Fairbanks and I. Macklin, Eds., MCIC-75-26, 1974.

3. C. G. McCreath, in "Third Conference on Gas Turbine Materials in a Marine Environment," Session V, Paper 2, University of Bath, England, Sept. 1976.

4. M. A. DeCrescente and N. S. Bornstein, Corrosion 24, 127 (1968).

5. N. S. Bornstein and M. A. DeCrescente, Trans. Metall. Soc. AIME 245, 1947 (1969).

6. J. A. Goebel and F. S. Pettit, Met. Trans. 1, 1943 (1970).

7. J. A. Goebel, F. S. Pettit, and G. W. Goward, Met Trans. 4, 261 (1973).

8. N. S. Bornstein, M. A. DeCrescente, and H. A. Roth, Met. Trans. 4, 1799 (1973).

9. P. M. Johnson, D. P. Whittle, and J. Stringer, Corr. Sci. 15, 721 (1975).

10. Y. Bourhis and C. St. John, Oxid. Met. 9, 507 (1975).

11. "Gas Turbine Materials Conference Proceedings," Naval Ship Engineering Center, Naval Air Systems Command, Washington, DC, 1972.

12. "Proceedings of the 1974 Gas Turbine Materials in the Marine Environment Conference," J. W. Fairbanks and I. Machlin, Eds., MCIC-75-27, 1974.

13. "Third Conference on Gas Turbine Materials in a Marine Environment," University of Bath, England, Sept. 1976.

14. K. H. Brinsmead and R. W. Kear, Fuel 35, 84 (1956).

15. R. H. Boll and H. C. Patel, J. Eng. Power 83, 451 (1961).

16. P. J. Jackson and H. C. Duffin, in "The Mechanism of Corrosion by Fuel Impurities," H. R. Johnson and D. J. Littler, Eds., p. 427, Butterworths, 1963.

17. J. Dunderdale and R. A. Durie, J. Inst. Fuel 37, 493 (1964).

18. S. A. Goldberg, J. J. Gallagher, and A. A. Orning, J. Eng. Power 90, 193 (1968).

19. W. D. Halstead and E. Raask, J. Inst. Fuel 42, 344 (1969).

20. W. D. Halstead and A. B. Hart, Central Electricity Generating Board Laboratory Memorandum No. RD/L/M 272 (1970).

21. R. J. Bishop and K. K. Cliffe, J. Inst. Fuel 42, 283 (1969).

22. A. J. B. Cutler, W. D. Halstead, J. W. Laxton, and C. G. Stevens, J. Eng. Power 93, 307 (1971).

23. C. A. Stearns, R. A. Miller, F. J. Kohl, and G. C. Fryburg, NASA TM X-73600 (1977).

24. G. C. Fryburg, R. A. Miller, C. A. Stearns, and F. J. Kohl, in "High Temperature Metal Halide Chemistry," D. L. Hildenbrand and D. D. Cubicciotti, Eds., p. 468, The Electrochemical Society Softbound Symp. Series, Vol. 78-1, Princeton, NJ, 1978: also NASA TM-73794 (1977).

25. C. A. Stearns, R. A. Miller, F. J. Kohl, and G. C. Fryburg, J. Electrochemical Society 124, 1145 (1977).

26. D. E. Rosner, First Semiannual Report on NASA Grant No. NSG-3169, Yale University, May 1978, NASA CR-159612.

27. D. E. Rosner, Second Semiannual Report on NASA Grant No. NSG-3169, Yale University, Nov. 1978, NASA CR-159613.

28. F. J. Kohl, G. J. Santoro, C. A. Stearns, G. C. Fryburg, and D. E. Rosner, J. Electrochemical Society 126, 1054 (1979); also NASA TM X-73683 (1977).

29. D. E. Rosner, B.-K. Chen, G. C. Fryburg, and F. J. Kohl, Combustion Science and Technology, in press.

30. D. E. Rosner, K. Seshadri, J. Fernandez de la Mora, G. C. Fryburg, F. J. Kohl, C. A. Stearns, and G. J. Santoro, in "Proceedings of the Tenth Materials Research Symposium: Characterization of High Temperature Vapors and Gases," National Bureau of Standards, Washington, DC, Sept. 1978, in press.

31. C. A. Stearns, F. J. Kohl, and G. C. Fryburg, in "Properties of High Temperature Alloys," Z. A. Foroulis and F. S. Pettit, Eds., p. 655, The Electrochemical Society Softbound Symposium Series, Vol. 77-1, Princeton, NJ, 1977; also NASA TM X-73476 (1976).

32. G. C. Fryburg, R. A. Miller, F. J. Kohl, and C. A. Stearns, J. Electrochemical Society 124, 1738 (1977); also NASA TM X-73599 (1977).

33. J. G. Smeggil and N. S. Bornstein, NASA CR-135348 (1977).

34. J. G. Smeggil and N. S. Bornstein, in "High Temperature Metal Halide Chemistry," D. L. Hildenbrand and D. D. Cubicciotti, Eds., p. 521, The Electrochemical Society Softbound Symposium Series, Vol. 78-1, Princeton, NJ, 1978.

35. J. G. Smeggil and N. S. Bornstein, J. Electrochemical Society 125, 1283 (1978).

36. J. G. Smeggil, N. S. Bornstein, and M. A. DeCrescente, in "Ash Deposits and Corrosion Due to Impurities in Combustion Gases," R. W. Bryers, Ed., p. 271, Hemisphere Publishing Corp., Washington, DC, 1978.

37. F. J. Kohl, C. A. Stearns, and G. C. Fryburg, in "Metal-Slag-Gas Reactions and Processes," Z. A. Foroulis and W. W. Smeltzer, Eds., p. 649, The Electrochemical Society Softbound Symposium Series, Princeton, NJ, 1975; also NASA TM X-71641 (1975).

38. JANAF Thermochemical Tables, Dow Chemical Co., Midland, MI, dated June 30, 1978 for $Na_2SO_4(g)$.

39. C. A. Stearns, F. J. Kohl, G. C. Fryburg, and R. A. Miller, in Proceedings of the Tenth Materials Research Symposium: Characterization of High Temperature Vapors and Gases," National Bureau of Standards, Washington, DC, Sept. 1978, in press; also NASA TM-73720 (1977).

40. S. Gordon and B. J. McBride, NASA SP-273 (1971).

41. J. W. Hastie, "High Temperature Vapors," p. 217, Academic Press, NY, 1975.

42. V. I. Hanby, J. Eng. Power 96, 129 (1974).

43. T. D. Brown, J. Inst. Fuel 39, 378 (1966).

44. A. B. Hedley, T. D. Brown, and A. Shuttleworth, J. Eng. Power 88, 173 (1966).

45. K. Ross, J. Inst. Fuel 38, 273 (1965).

46. R. A. Durie, J. W. Milne, and M. Y. Smith, Combustion and Flame 30, 221 (1977).

47. C. G. Root and A. R. Stetson, in Ref. 13, Session V, Paper 7.

48. L. F. Aprigliano, Report No. MAT-77-68, D. W. Taylor Ship R&D Center, 1977.

49. E. J. Felten and F. S. Pettit, Pratt and Whitney Quarterly Report, March 1, 1976 - May 31, 1976, NRL Contract No. N00173-76-C-0146.

50. T. J. Radzavich and F. S. Pettit, Pratt and Whitney Quarterly Report, June 1, 1976 - August 31, 1976, NRL Contract No. N00173-76-C-0146.

51. R. L. Jones and S. T. Gadomski, J. Electrochemical Society 124, 1641 (1977).

52. C. A. Stearns, F. J. Kohl, G. C. Fryburg, and R. A. Miller, in "High Temperature Metal Halide Chemistry," D. L. Hildenbrand and D. D. Cubicciotti, Eds., p. 555, the Electrochemical Society Softbound Symposium Series, Vol. 78-1, Princeton, NJ, 1978; also NASA TM-73796 (1977).

53. J. F. G. Condé and B. A. Wareham, in Ref. 12, p. 73.

54. P. Hancock, in Ref. 12, p. 225.

55. J. B. Johnson, J. R. Nicholls, R. C. Hurst, and P. Hancock, Corrosion Science 18, 527 (1978).

56. M. K. Hossain and S. R. J. Saunders, Oxidation Metals 12, 1 (1978).

57. D. W. McKee, D. A. Shores, and K. L. Luthra, J. Electrochemical Society 125, 411 (1978).

58. C. A. C. Sequeira and M. H. Hocking, J. Applied Electrochemistry 8, 179 (1978).

59. F. Mansfeld, N. E. Paton, and W. M. Robertson, Metallurgical Transactions 4, 321 (1973).

60. R. H. Barkalow and F. S. Pettit, "Degradation of Coating Alloys in Simulated Marine Environments," NRL Contract No. N-00173-76-C-0146, Final Report, June 15, 1978.

61. C. A. Stearns, F. J. Kohl, R. A. Miller, and G. C. Fryburg, NASA TM-79210 (1979).

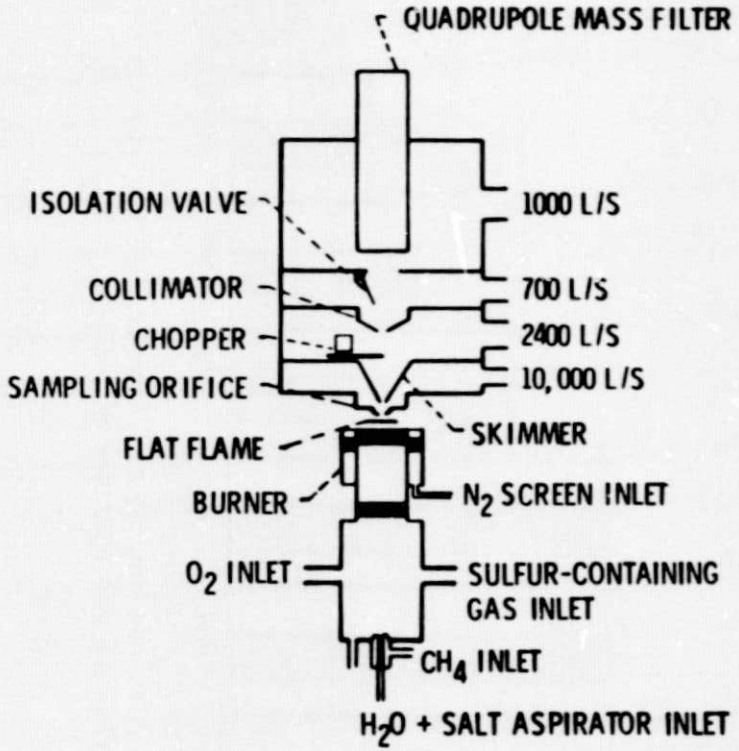

Figure 1. Schematic of the high pressure mass spectrometric flame sampling apparatus.

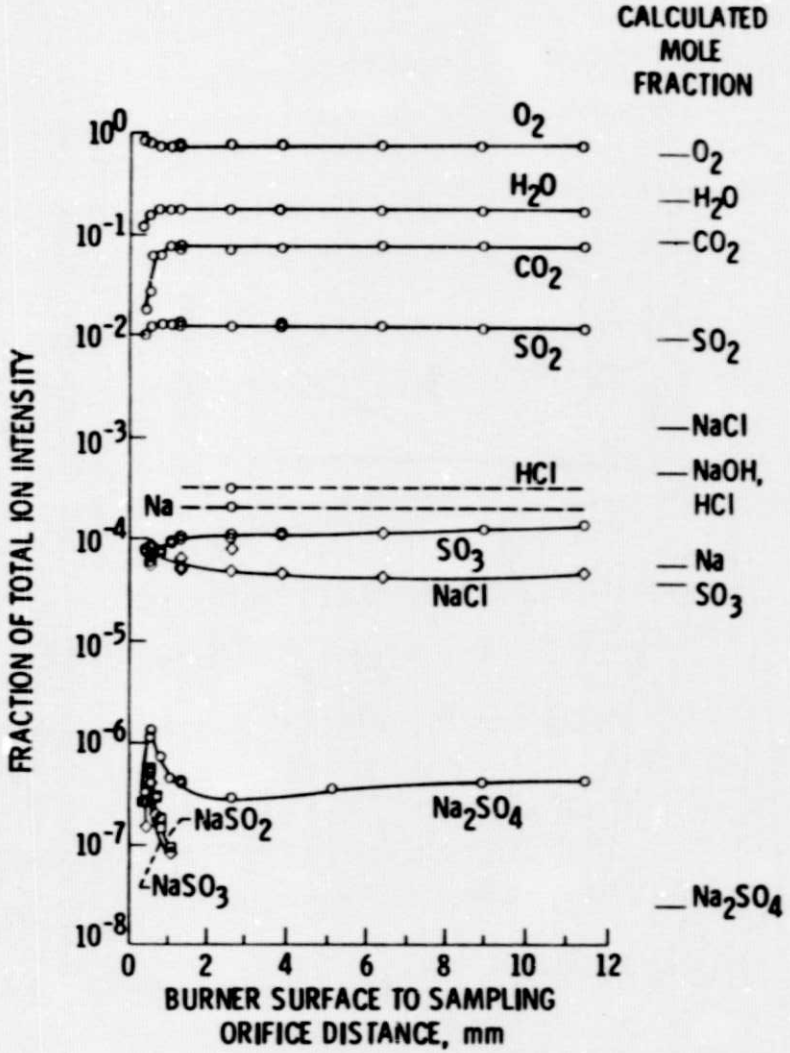

Figure 2. Composition profiles for CH_4-O_2-H_2O-NaCl-SO_2 flame. Reactants (mole %): 8.9CH_4, 84.1 O_2, 5.9 H_2O, 0.18 NaCl, and 0.92 SO_2. Fuel/oxidant mass ratio defined as 0.072. Calculated mole fractions refer to the adiabatic flame temperature of 2032K.

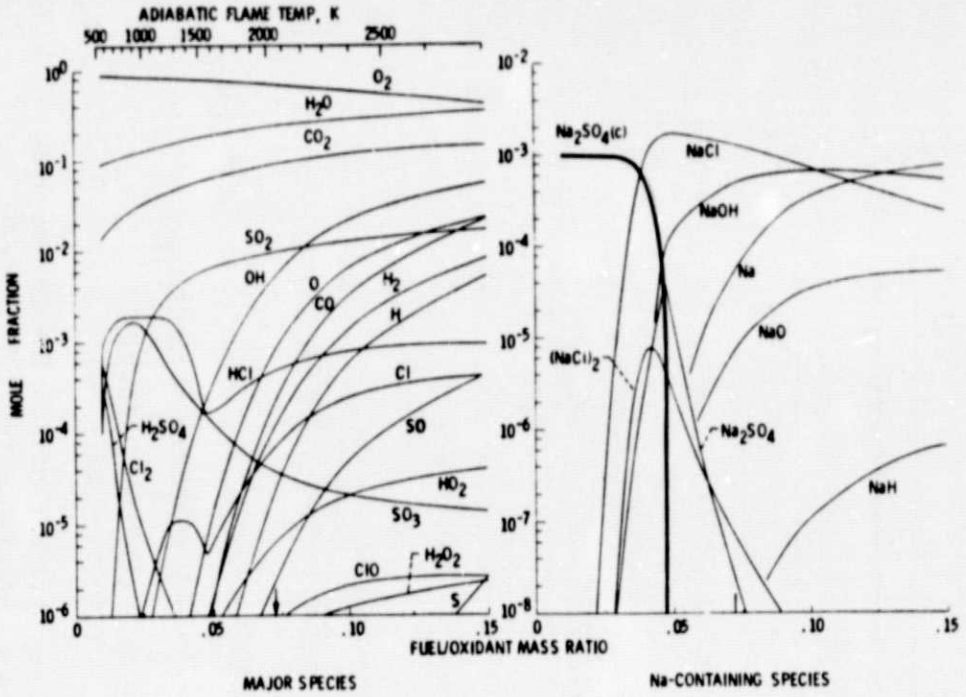

Figure 3. Equilibrium chemical composition for NaCl-SO_2 doped CH_4-O_2 flame. Arrow indicates the fuel/oxidant mass ratio of the experimental flame (reactant mole % - 8.9 CH_4, 84.1 O_2, 5.9 H_2O, 0.18 NaCl, and 0.92 SO_2).

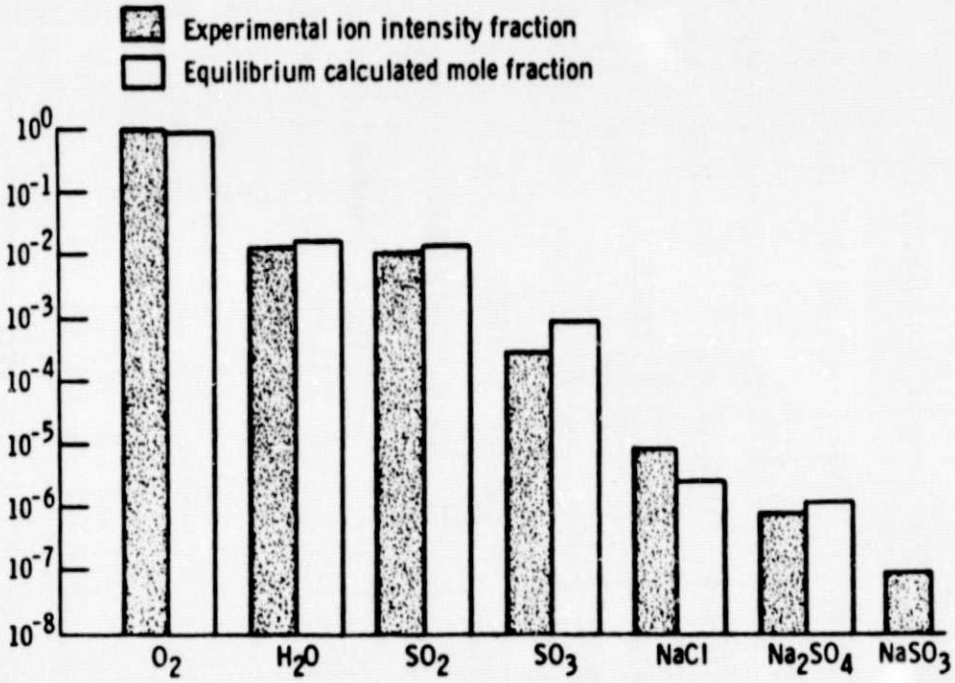

Figure 4. Comparison of measured and equilibrium calculated reaction products produced at 1413 K in a flowing gas mixture of NaCl(g) + SO_2(g) + H_2O(g) + O_2(g).

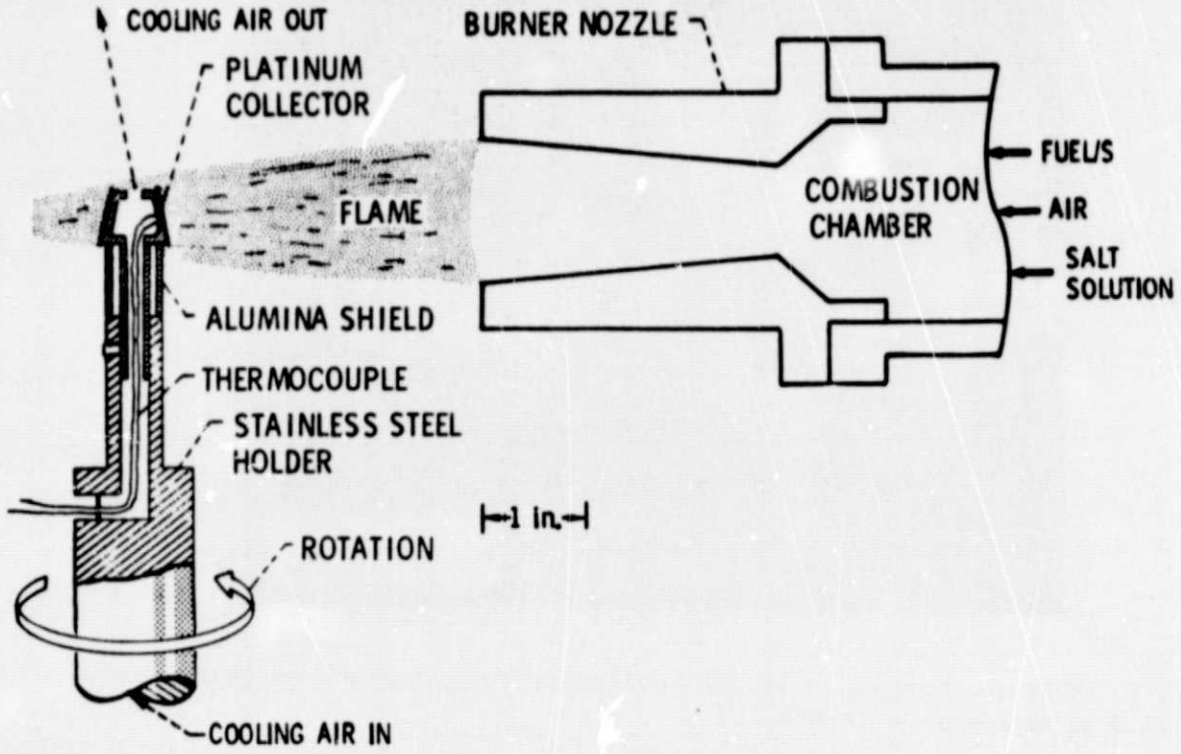

Figure 5. Schematic of the burner rig deposition apparatus.

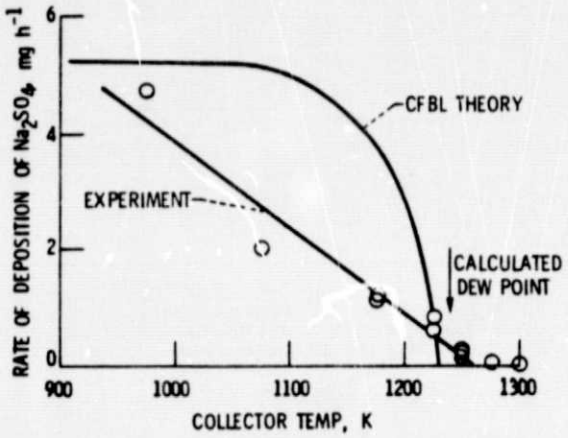

Figure 6. Comparison of experimental and calculated theoretical deposition rates of Na_2SO_4 from burner rig flame seeded with 11.3 wppm sea salt in the air and 0.038 wt. % sulfur in the fuel.

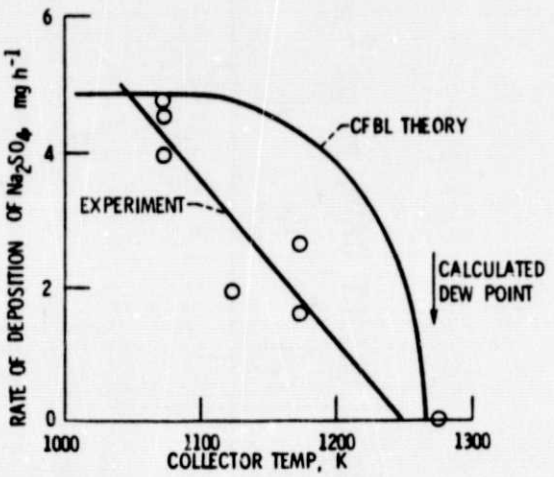

Figure 7. Comparison of experimental and calculated theoretical deposition rates of Na_2SO_4 from burner rig flame seeded with 8.0 wppm NaCl in the air and 0.25 wt. % sulfur in the fuel.

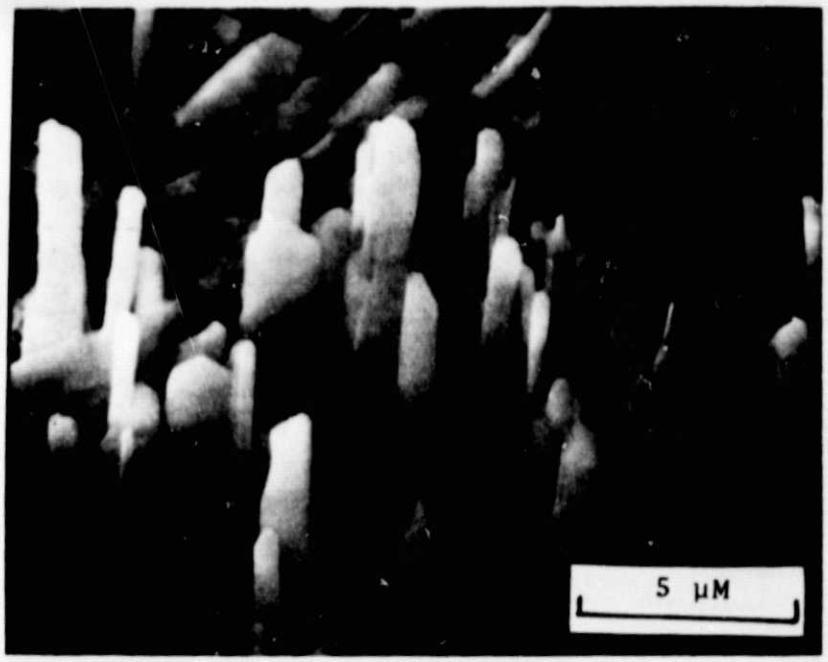

Figure 8. SEM micrograph of deposit collected from combustion gases seeded with 11.3 wppm sea salt in the air.

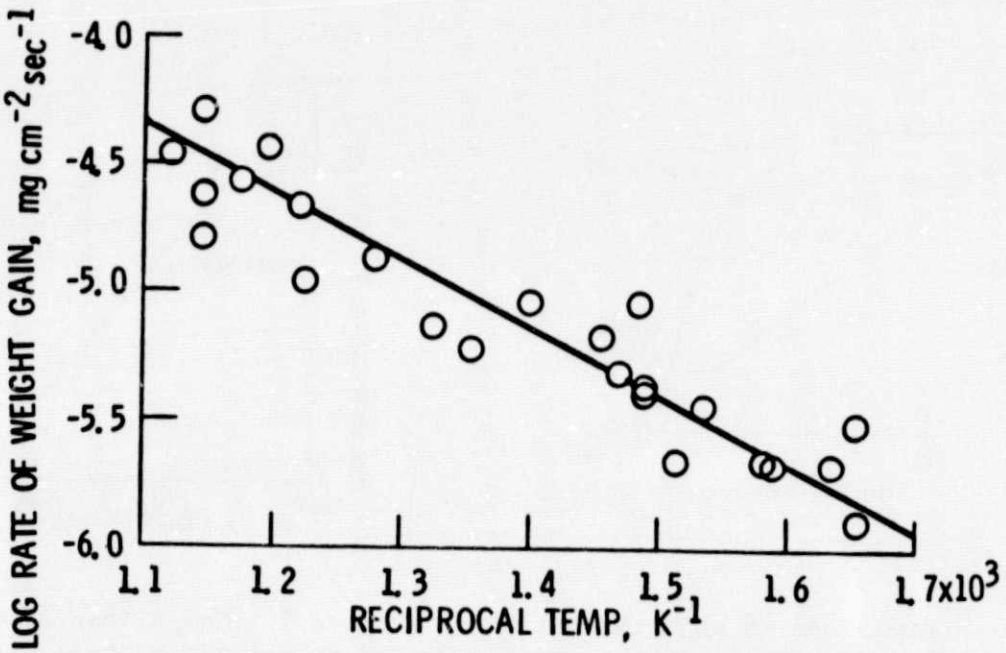

Figure 9. Gravimetric data for the conversion of single crystal NaCl(s) to Na_2SO_4(s). Conditions: 8 mole % SO_2 in flowing O_2(g) at 1 atmosphere.

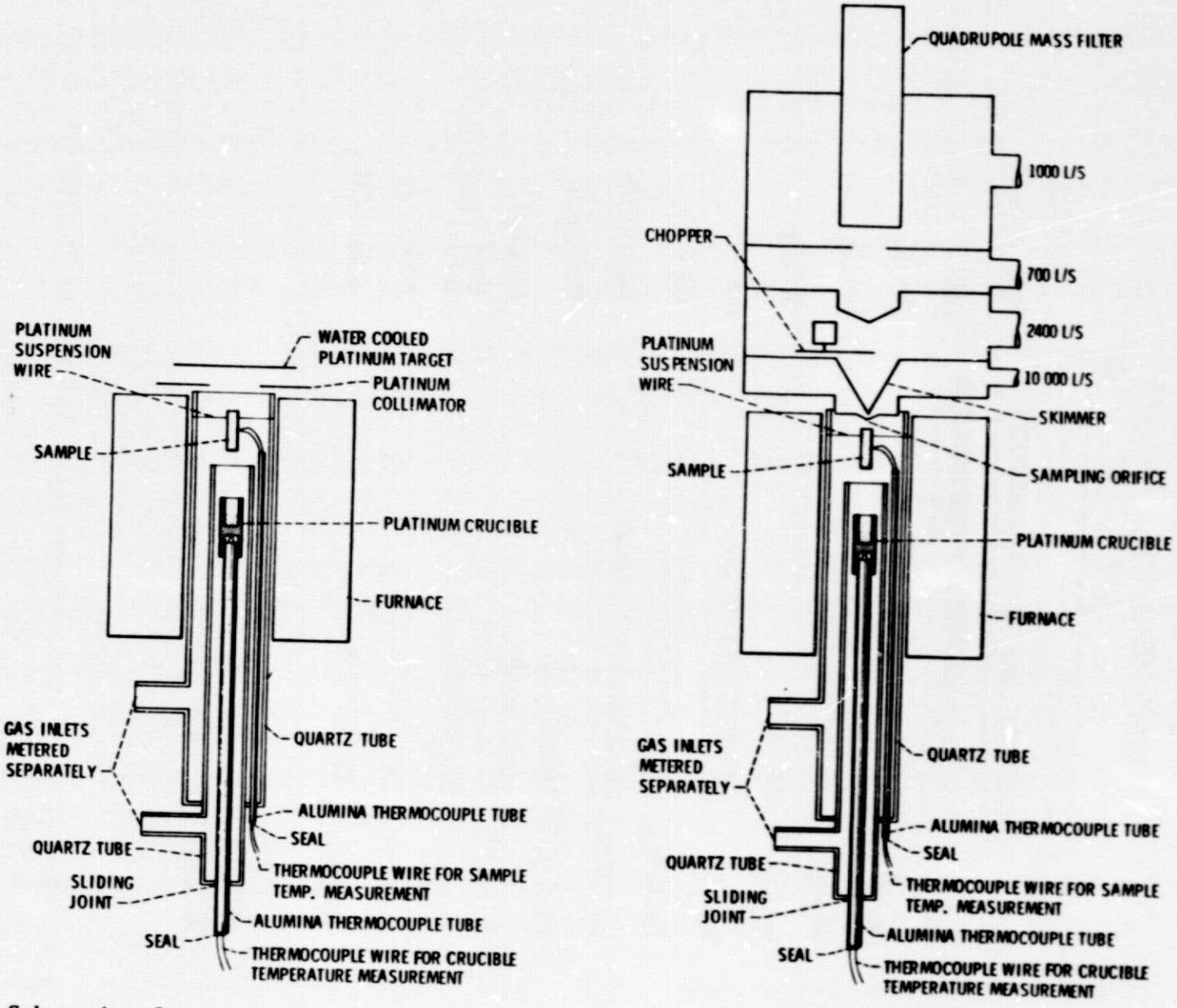

Figure 10. Schematic of vapor collection apparatus (left) and high pressure mass spectrometric sampler (right).

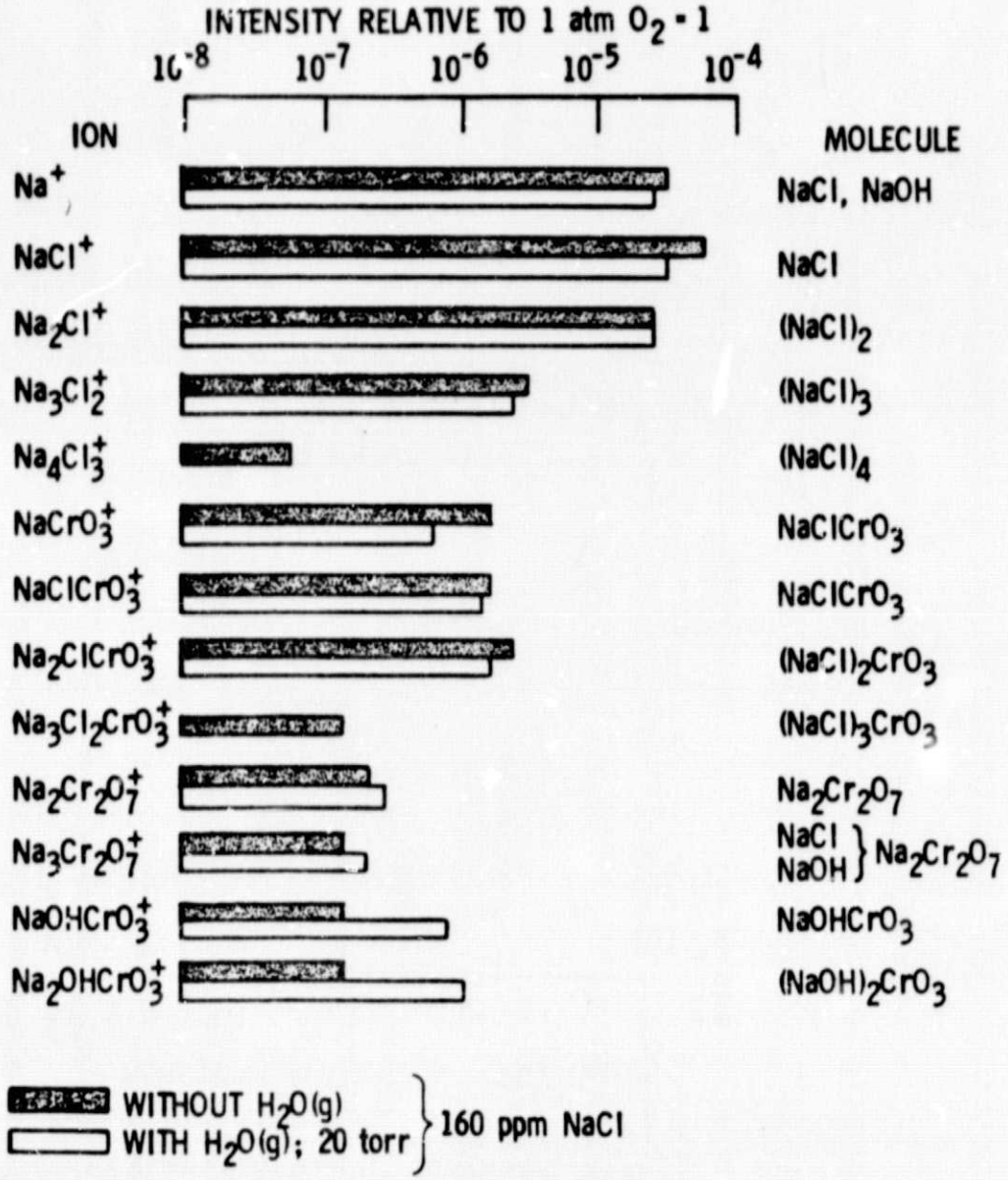

Figure 11. Mass spectrum of vapors over the $Cr_2O_3(c)$-$O_2(g)$-NaCl(g) system at 1020°C with and without added $H_2O(g)$.

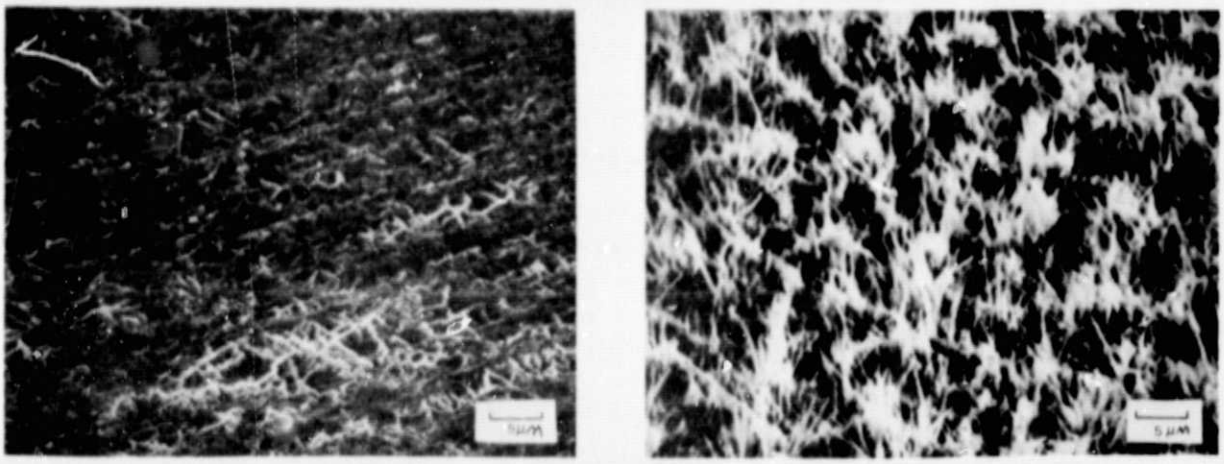

NiAl OXIDIZED IN AIR

NiAl OXIDIZED WITH 10 ppm NaCl VAPOR PRESENT

Figure 12. Micrographs of NiAl oxidized at 1050°C for 24 hours in air and in air with 10 ppm NaCl. (From Refs. 33 and 35).

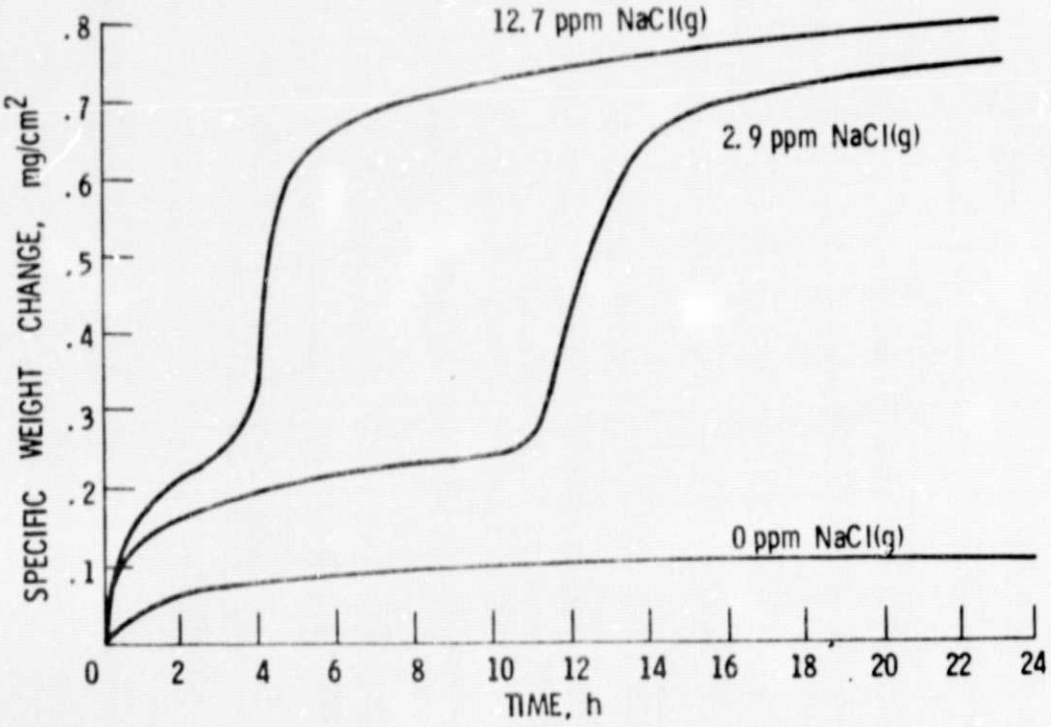

Figure 13. Oxidation of Ni-25Cr at 900°C in air and in air with NaCl(g) added. (From Refs. 33 and 34).

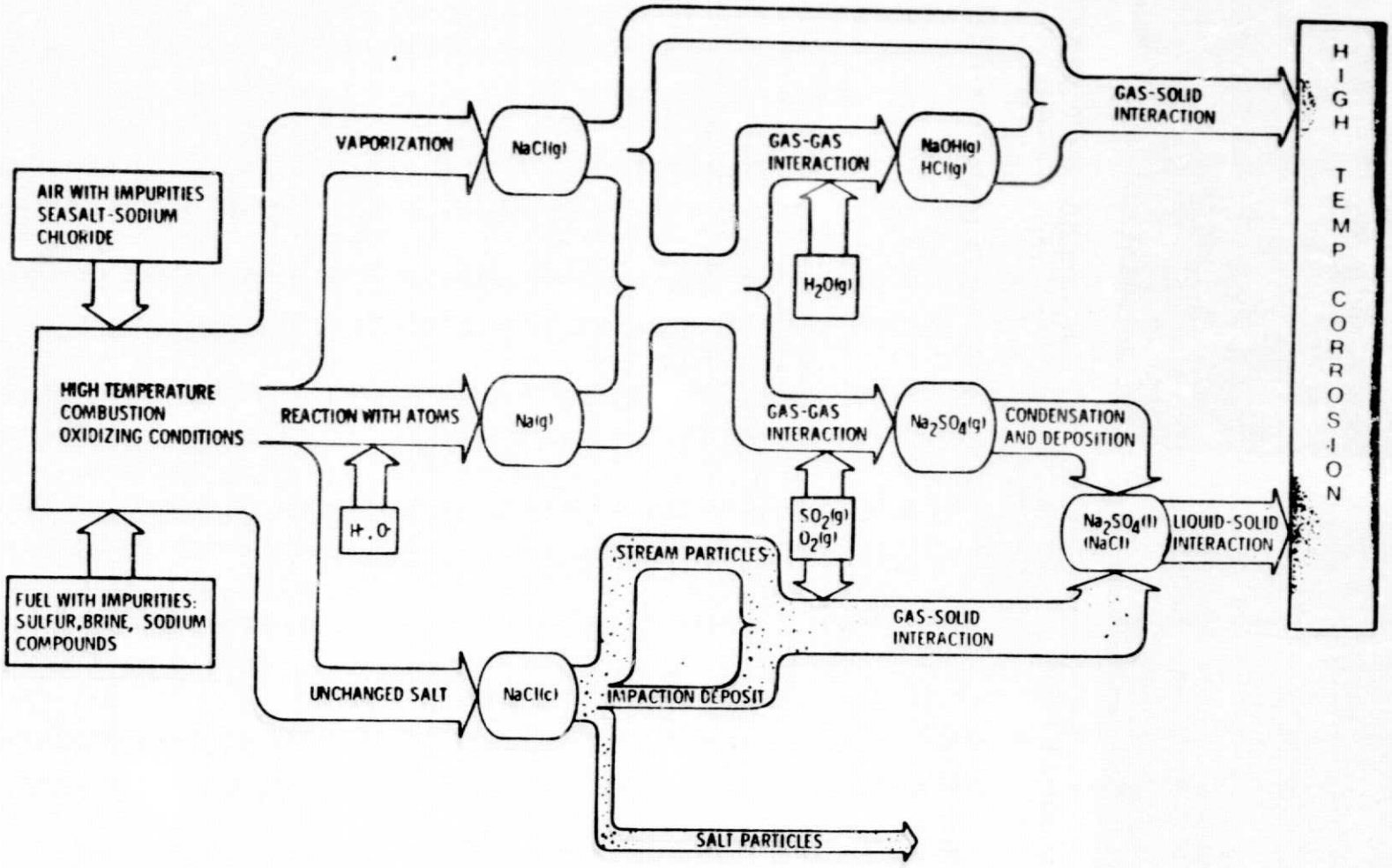

Figure 14. Behavior of NaCl in a turbine engine combustion gas environment.